Biochimica et Biophysica Acta, 776 (1984) 299–312
Elsevier

BBA 72243

FLUORESCENCE PROBES IN METASTATIC B16 MELANOMA MEMBRANES

FRIEDHELM SCHROEDER

Department of Pharmacology, University of Missouri-Columbia, School of Medicine, Columbia, MO 65212 (U.S.A.)

(Received March 7th, 1984)

Key words: Fluorescence polarization; Membrane structure; Rotational relaxation time; Lipid asymmetry; Metastasis; Melanoma; (Plasma membrane)

Fluorescence probe molecules, *trans*-parinaric acid and 1,6-diphenylhexatriene, were utilized to characterize the structure of plasma membranes, microsomes and mitochondria from B16 melanoma cells. High metastatic B16-F10 and low metastatic B16-F1 melanoma cell lines had markedly different membrane structures. The fluorescence polarization, fluorescence lifetime and limiting anisotropy of *trans*-parinaric acid were significantly lower ($P < 0.05$) in all three membrane fractions of the B16-F1 cell line than in the corresponding membranes of the B16-F10 cell line. These data indicated less restriction to rotational motion in the solid lipid domains of B16-F1 cell membranes preferentially sensed by *trans*-parinaric acid. The limiting anisotropy of both *trans*-parinaric acid and 1,6-diphenyl-1,3,5-hexatriene was significantly lower in the outer monolayer than the inner monolayer of the plasma membrane of B16-F1 cells but not in B16-F10 cells. A breakpoint in Arrhenius plots of fluorescence near 30–34°C indicated the presence of a phase separation that was assigned to the inner monolayer of the plasma membrane. However, no differences in this breakpoint temperature were noted between the B16-F1 and B16-F10 melanoma membranes. Thus, more fluid solid membrane domains and a distinct transbilayer fluidity difference were characteristic of plasma membranes from low metastatic B16-F1 melanoma cells in contrast to high metastatic B16-F10 melanoma cells.

Introduction

Considerable advances in our understanding of the metastatic process have recently been made possible through the use of tumor cell sublines of different metastatic potential [1,2]. Early investigations indicated that differences in cell surface membrane properties correlated with the metastatic properties of the tumor cell [3]. An interesting relationship between prostaglandin D_2 production, arachidonic acid release, inhibition of the immune response and altered membrane fluidity was recently postulated for high metastatic B16-F10 and low metastatic B16-F10 melanoma cells [4,5]. In addition, the lateral segregation of cell surface proteins was determined in both these cell lines by fluorescence photobleaching recovery [6]. Polymerized actin formed more aggregated patches in the cell surface of B16-F10 melanoma than B16-F1 melanoma cells. Increased membrane fluidity led to decreased adhesiveness of CHO tumor cells [7]. Most importantly, the oncogenic potential of a series of transformed C_3H 10 $T_{1/2}$ CL8 cells correlated directly with membrane fluidity [8]. Despite these findings, there have been no

Abbreviations: A, absorbance; CO, absorbance-corrected fluorescence; τ, lifetime; P, polarization; F, fractional fluorescence; X, mole fraction; R, rotational relaxation rate; r_∞, limiting anisotropy; r, steady-state anisotropy; r_0, anisotropy in the absence of rotational motion; TNBS, trinitrobenzenesulfonic acid.

detailed studies comparing plasma membrane structure and composition of the membrane lipids from high versus low metastatic cell lines. Elsewhere, we presented the lipid composition and distribution of phospholipid in membranes isolated from B16-F10 and B16-F1 melanoma cells [9]. Differences in cholesterol/phospholipid ratio phosphatidylcholine/ phosphatidylethanolamine ratio and in polyunsaturated fatty acid content were noted between the two cell lines. These findings therefore implied potential differences in membrane structure as well. Herein, are presented the results of fluorescence probe investigations on purified membranes from B16-F1 and B16-F10 melanoma cells in order to determine if structural differences exist between cellular membranes of these high and low metastatic cell lines.

Materials and Methods

Chemicals and fluorescence probe molecules. Trinitrobenzenesulfonic acid (TNBS) was purchased from Sigma Chemical Co. (St. Louis, MO). *trans*-Parinaric acid and 1,6-diphenylhexatriene were obtained from Molecular Probes (Junction City, OR) and Eastman Chemical Co. (Rochester, NY), respectively.

Cell culture and membrane isolation. B16-F10 and B16-F1 melanoma cells were cultured as described earlier [9]. Plasma membranes, microsomes and mitochondria were isolated and characterized also as described therein.

Fluorescence probe incorporation and instrumentation. trans-Parinaric acid and 1,6-diphenyl-1,3,5-hexatriene were incorporated into membranes at 1 : 100 mol ratios, unless otherwise specified as described earlier [10]. The computer-centered spectrofluorimeter, first developed by Holland and co-workers [12,13], was used to simultaneously determine absorbance, absorbance-corrected fluorescence, relative fluorescence efficiency and corrected fluorescence emission [14–17]. Light scattering was corrected by use of cutoff filters and narrow band passes.

Fluorescence lifetime, τ, and steady-state fluorescence polarization, P, were determined using a T format spectrofluorimeter [18], obtained from SLM (SLM 4800 Subnanosecond Spectrofluorimeter, SLM Instruments, Champaign-Urbana, IL), basically as described earlier [19]. In determination of polarization, light scattering was reduced by using narrow band passes in the excitation monochromator and cutoff filters in the emission monochromator. In addition, samples were serially diluted and polarization was measured extrapolated to zero absorbance [20,21]. All fluorescence lifetimes were measured with the excitation polarizer set at 0° and the emission polarizer set at 55° in order to eliminate Brownian motion as a determinant of apparent lifetime. Fluorescence lifetimes were simultaneously measured relative to a reference solution of dimethyl-*p*-bis[2-(5-phenyloxazolyl)]benzene (i.e., dimethyl POPOP) in absolute ethanol as described previously [22]. Multiple lifetimes were resolved by Weber's closed-form heterogeneity analysis [23] using a PDP-8E Computer (Digital Eq. Co., Maynard, MA). This program also provides fractional fluorescence values. The latter can be converted to mole fractions according to:

$$X_i = (F_i/\tau_i)/(\Sigma_j F_j/\tau_j) \quad (1)$$

where X_i, F_i and τ_i are the mole fraction, fractional fluorescence and lifetime of component i. The excitation wavelengths for *trans*-parinaric acid and 1,6-diphenyl-1,3,5-hexatriene in fibroblast membranes were 313 and 362 nm, respectively; fluorescence emission was monitored at 415 and 424 nm, respectively.

Differential polarized phase fluorometry was used to obtain the rotational rate and limiting anisotropy of fluorescence probes in membranes [24]. Determination of rotational relaxation times or microviscosity according to steady-state techniques [25,26], was not used, since the steady-state anisotropy used in these calculations is comprised to two components: r_∞, the limiting anisotropy, which is determined primarily by the degree to which the rotations are hindered, and R, the rotational rate [24,27,28]. Instead, we utilized the method of Lakowicz et al. [24] to obtain the limiting anisotropy and rotational rate directly as follows:

$$r_\infty = r + (r - r_0)/6R\tau \quad (2)$$

where r_∞ is the limiting anisotropy, r is the steady-state anisotropy, r_0 is the anisotropy in the

absence of rotational motion, τ is the lifetime and R is the rotational rate in radians/s. The relaxation rate expressed in ns is equivalent to $(6R)^{-1}$. The r_0 for diphenylhexatriene and *trans*-parinaric acid is 0.392 and 0.390, respectively [24,29]. The value for R can be obtained from differential polarized phase measurements as follows [24]:

$$(m \tan \Delta)(2R\tau)^2 + (C \tan \Delta - A)(2R\tau) + (D \tan \Delta - b) = 0 \quad (3)$$

where $A = 3B = w\tau(r_0 - 4)$, $C = (1/3)(2r - 4r^2 + 2)$, $D = (1/9)(m + m_0 w^2 \tau^2)$, $m = (1 + 2r)(1 - r)$. The steady-state anisotropy, r, is equivalent to $[2P/(3 - P)]$, where P is the polarization. In biological membranes, the r is dependent primarily on the range of motion rather than the rate, and alterations in membrane components such as cholesterol, proteins, etc., largely reflect alterations in range of motion rather than rate [27,30,31]. Such calculations can also be performed with probe molecules that have multiple lifetimes (i.e., *trans*-parinaric acid) by using Weber's Law for the additivity of polarization anisotropy [32]. Weber's Law of anisotropy additivity requires intensity weighting for the addition of fractional anisotropies. Fractional fluorpescence intensities (F_1 and F_2) are obtained from the multiple lifetime analysis as described above. Similarly, the contribution of probe molecule in several lipid domains with different lifetimes to an average or τ_{mix} can be obtained from $\tau_1 F_1$ plus $\tau_2 F_2$. Thus, an r_{mix} obtained from diifferential-polarized phase fluorescence measurements and a τ_{mix} may be inserted into Eqn. 2 to provide an R_{mix} or average rotational relaxation time. The latter is only an approximation and subject to the assumption that r_∞ is the same in both lipid environments. Another limitation is the error involved in determination of lifetimes and fractional fluorescence intensities with the phase method.

Sample temperature was varied with an Exocal 100, Endocal 850 and ETP-3 Temperature Programmer system (Neslab Inst., Portsmouth, NH). Sample temperature was monitored with a thermocouple placed directly in the cuvette and a WR-700 Digital Thermometer (Kernco Inst., El Paso, TX). All detections represent the average of 40 values taken in several milliseconds for each sample at each temperature. All values presented represent the mean of three samples. All samples were studied in aqueous phosphate-buffered saline (50 μg protein/ml). All fluorescence Arrhenius plots were heating scans, although cooling scans were performed and similar data were obtained.

Trimitrobenzenesulfonic acid labelling. TNBS labelling of B16 melanoma cells cultured in monolayer was performed at 4 or at 37 °C as described earlier [33]. This method has been used to trinitrophenylate the external surface of intact plasma membrane under nonpenetrating conditions (4 °C) or both membrane surfaces under penetrating conditions (37 °C) for fibroblasts [33–34], synaptosomes [35] and phagosomes [36–37]. The basic method is a modification of that developed earlier by the laboratories of Marinetti et al. and Litman et al. [38–40]. The asymmetric distribution of aminophospholipid was determined as described earlier [33]. The difference in transbilayer structure was determined also as described earlier [10,41–42,19].

Results

Spectral characteristics of trans-parinaric acid and 1,6-diphenylhexatriene in B16 melanoma membranes

The ultraviolet absorption and fluorescence properties of *trans*-parinaric acid in isolated plasma membranes from B16-F10 melanoma cells indicated characteristic excitation maxima at 290, 303 and 318 nm, while a broad emission maximum occurred near 410 nm. The excitation and emission transitions were well-separated, such that, there was little overlap of emission and excitation spectra. Similar spectral properties were obtained with *trans*-parinaric acid in the microsomes and mitochondria, except that the ratio of absorbance-corrected fluorescence of excitation peaks at 318/292 nm from microsomes was 27% greater than that of plasma membranes from B16-F10 melanoma cells (Table I). A higher ratio indicates that the microenvironment sensed by the *trans*-parinaric acid in the microsomes was slightly more polar or had a higher dielectric constant (see Table I of Ref. 43, Table I of Ref. 19, and Ref. 15). Similar results were obtained with *trans*-

TABLE I

SPECTRAL CHARACTERIZATION OF PROBE MOLECULES IN MEMBRANES OF B-16 MELANOMA VARIANTS

Spectral characteristics of *trans*-parinaric acid and 1,6-diphenyl-1,3,5-hexatriene were determined in membranes of B-16 melanoma variants as described in Materials and Methods.

Probe molecule	Parameter	Variant	
		F1	F10
Plasma membranes			
trans-Parinaric acid	excitation maxima [a]	320,306,292	318,303,290
	emission maximum [a]	410	410
	CO_{318}/CO_{290}	1.22 ± 0.06 [b,c]	0.91 ± 0.05 [b,c]
1,6-Diphenyl-1,3,5-hexatriene	excitation maxima	376,356,342	377,356,344
	emission maxima	402,425,450	400,424,445
	CO_{373}/CO_{339}	0.97 ± 0.03	0.92 ± 0.02
Microsomes			
trans-Parinaric acid	excitation maxima	318,305,290	317,302,288
	emission maximum	410	415
	CO_{318}/CO_{290}	1.53 ± 0.04 [b,c]	1.17 ± 0.07 [b,c]
1,6-Diphenyl-1,3,5-hexatriene	excitation maxima	375,356,340	378,357,342
	emission maxima	402,427,450	400,425,447
	CO_{373}/CO_{339}	1.03 ± 0.38	0.98 ± 0.04
Mitochondria			
trans-Parinaric acid	excitation maxima	318,304,290	321,306,293
	emission maximum	410	410
	CO_{318}/CO_{290}	1.13 ± 0.07	1.12 ± 0.06
1,6-Diphenyl-1,3,5-hexatriene	excitation maxima	375,358,342	375,358,340,328
	emission maxima	399,425,451	398,425,214
	CO_{373}/CO_{339}	0.98 ± 0.02	1.01 ± 0.04

[a] Excitation and emission maxima are given in nm.
[b] $P < 0.05$ by student's *t*-test (n = 3) between F1 and F10.
[c] $P < 0.05$ between membranes in a single cell line.

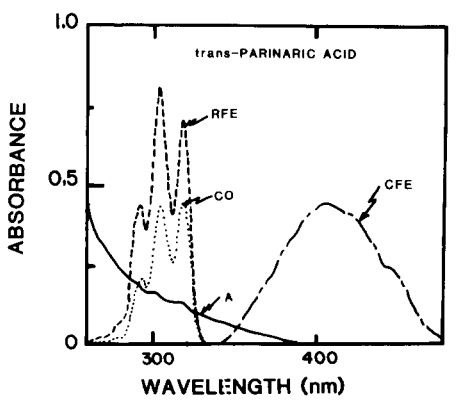

Fig. 1. Fluorescence excitation and emission spectra of *trans*-parinaric acid in B16-F10 melanoma plasma membranes. *trans*-Parinaric acid was incorporated into isolated plasma membranes (50 μg protein/ml phosphate-buffered saline) and fluorescence spectra were determined as described in Materials and Methods. RFE, relative fluorescence emission; CFE, corrected fluorescence emission; CO, absorbance-corrected fluorescence; *A*, absorbance.

parinaric acid incorporated into plasma membranes, microsomes and mitochondria for B16-F1 melanoma cells, except that the ratio of CO_{318}/CO_{290} was 34 and 31% higher in plasma membranes and microsomes, respectively, from B16-F1 melanoma than in B16-F10 melanoma cells. These data were consistent with the fluorescent fatty acid, *trans*-parinarate, being located in a membrane microenvironment of higher dielectric or polarity in B16-F1 than in B16-F10 melanoma plasma membranes and microsomes.

Fluorescence characteristics of 1,6-diphenylhexatriene in plasma membranes of B16-F10 melanoma cells displayed excitation maxima near 344, 356 and 377 nm, while emission maxima were resolved near 400, 424 and 445 nm (Fig. 2). The shapes of the absorbance-corrected fluorescence excitation and emission curves approached a mirror-image relationship. The excitation and emis-

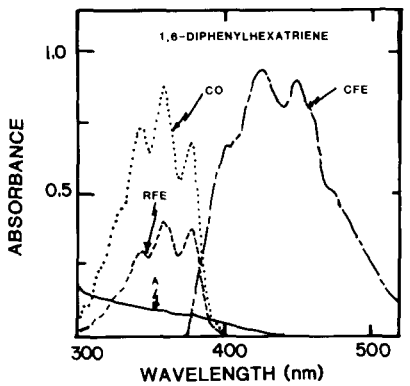

Fig. 2. Fluorescence excitation and emission spectra of 1,6-diphenylhexatriene in B16-F10 melanoma plasma membranes. All conditions were as specified in the legend of Fig. 1, except that 1,6-diphenylhexatriene was used instead of *trans*-heparinaric acid. Abbreviations as in Fig. 1.

sion transitions overlapped in the area of 370–405 nm. The spectral properties of 1,6-diphenylhexatriene in microsomes and mitochondria of B16-F10 melanoma cells were similar to those of the plasma membranes. No difference in probe microenvironment was apparent between the subcellular membranes. In addition, the fluorescence characteristics of 1,6-diphenylhexatriene in membranes of B16-F1 melanoma cells displayed no significant diffrence from those of B16-F10 melanoma cell membranes.

Fluorescence probe properties in B16 melanoma membranes

The fluorescence properties of *trans*-parinaric acid in plasma membranes, microsomes and mitochondria of B16 melanoma cells indicated the presence of a more rigid lipid microenvironment in the B16-F10 melanoma cell line than in the B16-F1 line (Table II). In all cases, the limiting anisotropy of *trans*-parinaric acid was significantly ($P < 0.05$) greater in the plasma membranes (9%), microsomes (9%) and mitochondria (13%) of B16-F10 melanoma cells than in those from B16-F1 melanoma cells. The limiting anisotropy is sensitive to rotational constraint imposed on the *trans*-parinaric acid by the surrounding lipid environment. In contrast, the rotational rate was unchanged near 2 ns. The larger limiting anisotropies in B16-F10 membranes, calculated as described in Eqns. 2 and 3, was primarily due to increases in both fluorescence polarization and fluorescence lifetime. The two fluorescence lifetimes of *trans*-parinaric acid near 3 and 15 ns represented the probe motion in fluid and solid membrane domains, respectively [16,17,44,45]. The lifetime component associated with the solid membrane domains (τ_2) was significantly longer in the B16-F10 melanoma membranes than in B16-F1 melanoma membranes.

Because *trans*-parinaric acid shows a nearly 4-fold selective partition into solid lipid domains [16,17,44,45], a second fluorescence probe molecule that does not display such a preference was chosen to determine if the results obtained with *trans*-parinarate represented properties of a select microenvironment in B16 melanoma membranes or if these results reflect the membranes as a whole. The fluorescence probe molecule, 1,6-diphenylhexatriene, displayed only a single lifetime component in B16 melanoma membranes (Table III). In contrast to the results obtained with *trans*-parinaric acid, the fluorescence polarization, lifetime, limiting anisotropy and rotational relaxation time of 1,6-diphenylhexatriene were not significantly different between membranes of B16-F10 and B16-F1 melanoma cell lines. Mitochondrial membranes had less restriction to the 1,6-diphenyl-1,3,5-hexatriene rotational movement (r_∞) than the plasma membranes or microsomes.

TNBS labelling of B16 melanoma plasma membranes

In order to determine if a difference in structure exists across the outer and inner monolayer of the plasma membrane as it does for other tumorigenic cell [46] surface membranes [10,41,42], TNBS labelling was performed to provide a suitable fluorescence-quenching agent covalently linked to one or both sides of the plasma membrane bilayer. First, however, the labelling behavior of TNBS was determined to ascertain the degree of penetration of TNBS into the cell and to determine if major structural damage affecting membrane enzyme functions occurred. The effect of the chemical-labelling reagent on the activities of membranous enzymes is shown in Table IV. TNBS treatment of B16-F1 and B16-F10 melanoma cells under nonpenetrating conditions at 4°C did not

TABLE II

FLUORESCENCE CHARACTERISTICS OF *trans*-PARINARIC ACID IN B-16 MELANOMA CELL VARIANTS

Fluorescence characteristics of *trans*-parinaric acid were determined in B-16 melanoma membranes as described in Materials and Methods. Values represent the mean ± S.E. ($n = 3$).

Parameter	Membrane fraction					
	Plasma membrane		Microsomes		Mitochondria	
	F1	F10	F1	F10	F1	F10
Absorbance	0.164 ± 0.012	0.118 ± 0.011	0.124 ± 0.006	0.134 ± 0.008	0.144 ± 0.013	0.137 ± 0.013
Corrected-fluorescence	50 ± 4	35 ± 8	15 ± 3	23 ± 4	24 ± 4	32 ± 7
Relative fluorescence efficiency	114 ± 13	130 ± 28	50 3	73 ± 13	95 ± 17	111 ± 27
Polarization	0.309 ± 0.005 [a]	0.324 ± 0.0022 [a]	0.2960 ± 0.004 [a]	0.310 ± 0.003 [a]	0.297 ± 0.004 [a]	0.318 ± 0.002 [a]
Lifetime γ_1 (ns)	3.0 ± 0.6	3.6 ± 0.4	0.296 ± 0.004 [a]	4.2 ± 0.3 [a]	2.7 ± 0.1	3.7 ± 0.6
Lifetime γ_2 (ns)	12.7 ± 0.8 [a]	15.4 ± 0.4 [a]	12.0 ± 0.6 [a]	16.4 ± 0.4 [a]	10.8 ± 0.4 [a]	15.7 ± 0.7 [a]
Fractional fluorescence F_1	0.31 ± 0.05	0.28 ± 0.02	0.31 ± 0.03	0.44 ± 0.02	0.36 ± 0.05	0.43 ± 0.06
Fractional fluorescence F_2	0.69 ± 0.05	0.72 ± 0.02	0.69 ± 0.03	0.56 ± 0.02	0.64 ± 0.05	0.57 ± 0.06
Mole fraction X_1	0.65 ± 0.05	0.63 ± 0.02	0.67 ± 0.03	0.75 ± 0.02	0.60 ± 0.05	0.76 ± 0.06
Mole fraction X_2	0.35 ± 0.05	0.37 ± 0.02	0.33 ± 0.03	0.25 ± 0.02	0.31 ± 0.05	0.24 ± 0.06
Limiting anisotropy	0.196 ± 0.003 [a]	0.213 ± 0.001 [a]	0.181 ± 0.002 [a]	0.197 ± 0.002 [a]	0.182 ± 0.002 [a]	0.206 ± 0.001 [a]
Average rotational relaxation time (ns)	2.04 ± 0.13	2.38 ± 0.20	2.02 ± 0.15	2.31 ± 0.21	1.75 ± 0.24	2.14 ± 0.29

[a] $P < 0.050$ as determined by Student's t-test.

TABLE III

FLUORESCENCE CHARACTERISTICS OF 1,6-DIPHENYLHEXATRIENE IN B-16 MELANOMA CELL VARIANTS

Fluorescence characteristics of 1,6-diphenylhexatriene were determined in B-16 melanoma membranes as described in Materials and Methods. Values represent the mean ± S.E. ($n = 3$).

Parameter	Membrane fraction					
	Plasma membrane		Microsomes		Mitochondria	
	F1	F10	F1	F10	F1	F10
Absorbance	0.08 ± 0.011	0.044 ± 0.007	0.075 ± 0.015	0.058 ± 0.005	0.066 ± 0.002	0.074 ± 0.009
Corrected-absorbance	53 ± 6	52 ± 6	39 ± 3	36 ± 6	21 ± 5	52 ± 11
Relative fluorescence efficiency	297 ± 62	307 ± 51	242 ± 41	188 ± 23	139 ± 21	321 ± 42
Polarization P	0.307 ± 0.007	0.313 ± 0.006	0.311 ± 0.001	0.305 ± 0.003	0.301 ± 0.004	0.286 ± 0.010
Lifetime (ns)	8.7 ± 0.4	9.1 ± 0.5	8.5 ± 0.4	8.5 ± 0.1	7.4 ± 0.2	8.5 ± 0.5
Limiting anisotropy	0.191 ± 0.004	0.194 ± 0.004	0.195 ± 0.001	0.188 ± 0.006	0.177 ± 0.002	0.168 ± 0.006
Rotational relaxation time (ns)	1.96 ± 0.10	2.23 ± 0.15	1.92 ± 0.14	1.96 ± 0.10	2.01 ± 0.07	2.01 ± 0.072.01 ± 0.26

TABLE IV

EFFECTS OF TNBS ON B16 MELANOMA ENZYMES

The B-16 melanoma variants were cultured and treated with a chemical-labeling reagent, TNBS, under nonpenetrating (4°C) conditions as described in Materials and Methods. Enzyme activities (nmol/min per mg protein) were determined. Values represent the mean ± S.E ($n = 4–7$).

Cell variant	Enzyme	Trinitrobenzenesulfonic acid	
		−	+
B16-F1	(Na^+-K^+)-ATPase	23.3 ± 5.7	21.7 ± 6.7
	Mg^{2+}-ATPase	28.3 ± 7.3	23.3 ± 13.4
	5′-nucleotidase	16.1 ± 2.5	13.2 ± 5.4
	NADPH-dependent cytochrome *c* reductase	87.0 ± 3.3	96.1 ± 8.3
	succinate-dependent cytochrome *c* reductase	89.6 ± 11.6	107.9 ± 26.1
B16-F10	$(Na^+ + K^+)$-ATPase	27.7 ± 3.9 [a]	10.4 ± 3.2 [a]
	Mg^{2+}-ATPase	16.2 ± 6.0	15.1 ± 6.7
	5′-nucleotidase	13.6 ± 2.1 [a]	26.1 ± 4.0 [a]
	NADPH-dependent cytochrome *c* reductase	68.6 ± 7.4	91.2 ± 12.0
	succinate-dependent cytochrome *c* reductase	162.4 ± 16.9	157.8 ± 7.3

[a] $P < 0.05$ as determined by Student's *t*-test.

significantly alter any of the intracellular (microsomal or mitochondrial) membrane enzyme activities of B16-F1 cells. In contrast, treatment of B16-F10 melanoma cells under nonpenetrating conditions with TNBS decreased the activity of $(Na^+ + K^+)$-ATPase by 62%, but the activity of 5′-nucleotidase was increased 2-fold. This increase was not due to enhanced exfoliation of 5′-nucleotidase in B16-F1 cells by treatment with TNBS. The ratio of soluble to particulate 5′-nucleotidase ($33\,000 \times g$ supernatant/$33\,000 \times g$ pellet) in the membrane preparation was not altered by treatment of either B16-F1 or B16-F10 cells with TNBS (data not shown). In both cases, approx. 80% of the enzyme was in the supernatant, while 20% was particulate.

The percentage of trinitrophenylated aminophospholipids in the plasma membrane under nonpenetrating reaction conditions with TNBS indicated the degree of exposure of these lipids in the outer monolayer of the cell plasma membrane [33]. Both cell lines showed that 5–7% and 15–23% of their phosphatidylethanolamine and phosphatidylserine reacted with TNBS, respectively (Table V). If the reagent had penetrated the cell surface membrane at 4°C, extensive trinitrophenylation of microsomal and mitochondrial phospholipids would be expected. However, this was not the case. Less than 2% of phosphatidylethanolamine and phosphatidylserine, respectively, were trinitrophenylated in the intracellular organelles. This small degree of trinitrophenylation may in part be due to cross-contamination of microsomes and mitochondria with cell surface membrane fragments. When cells were treated with TNBS at 4°C, the trinitrophenylphosphatidylethanolamine and trinitrophenylphosphatidylserine retained their distribution in the membrane. Warming the cells to 24, 37, or 45°C and then re-exposing to TNBS did not result in appearance of additional trinitrophenylated phosphatidylethanolamine or phosphatidylserine. Thus, the fluorescence-quenching sites described in the following section remained on the outer surface. Under penetrating reaction conditions (37°C), greater than 90% of all cellular aminophospholipids were trinitrophenylated and subcellular membrane enzymes were inhibited. These data, combined with the lack of intracellular membrane enzyme inhibition, indicate that at 4°C, the chem-

TABLE V

PHOSPHOLIPID DISTRIBUTION IN B16 MELANOMA VARIANTS

B16 melanoma variants were treated with TNBS at 4°C as described in Materials and Methods. Values represent the mean ± S.E. ($n = 3$). The percent trinitrophenylation is calculated as follows:

$$\text{percent labeled} = \frac{(\%\ \text{trinitrophenylated phospholipid})}{(\%\ \text{trinitrophenylated phospholipid} + \text{unreacted phospholipid})}$$

Phospholipid (mol %)	B16 melanoma variant	Cell homogenate	Plasma membrane	Microsomes	Mitochondria
Trinitrophenylated phosphatidylethanolamine	F1	9.6 ± 3.9	7.3 ± 2.4	1.2 ± 1.4	0.9 ± 0.9
	F10	6.4 ± 1.6	4.9 ± 0.3	1.0 ± 1.1	0.8 ± 0.4
Trinitrophenylated phosphatidylserine	F1	26.4 ± 6.9	15.5 ± 2.9	1.2 ± 0.4	1.3 ± 0.3
	F10	20.1 ± 7.7	23.5 ± 6.3	1.1 ± 0.4	1.0 ± 0.5

ical-labelling reagent, TNBS, did not leak into the cell. In summary, the asymmetric distribution of aminophospholipids did not appear to differ significantly between B16-F1 and B16-F10 melanoma cells.

Fluidity gradients in B16 melanoma plasma membranes

Under conditions in which TNBS did not permeate the cell membrane, the outer monolayer of B16 melanoma plasma membranes was labelled

TABLE VI

EFFECT OF TNBS ON PLASMA MEMBRANE FLUORESCENCE OF B-16 MELANOMA CELLS

Fluorescence parameters were determined on isolated plasma membranes of B-16 melanoma cells before and after treatment of cells under nonpenetrating conditions (4°C) with TNBS as described in Materials and Methods. Lifetime and limiting anisotropy, for 1,6-diphenylhexatriene were determined as described in Materials and Methods. For *trans*-parinaric acid, average lifetime (γ_{mix}) and outer monolayer limiting anisotropy were determined according to Weber's law of additivity of anisotropy weighing by fractional intensities. Values represent the mean ± S.E. ($n = 3$).

Parameter	TNBS	*trans*-Parinaric acid		1,6-Diphenylhexatriene	
		F1	F10	F1	F10
Corrected fluorescence	−	50 ± 2	35 ± 8	73 ± 6	52 ± 6
	+	41 ± 3	23 ± 4	61 ± 6	40 ± 1
Lifetime, γ or γ_{mix}	−	9.8 ± 8 [a]	12.1 ± 4 [a]	8.7 ± 0.4	9.1 ± 0.5
	+	13.1 ± 1.1	12.1 ± 0.3	9.5 ± 0.3	8.3 ± 0.2
Polarization, P	−	0.305 ± 0.004 [a,b]	0.324 ± 0.002 [a]	0.306 ± 0.003 [b]	0.316 ± 0.006
	+	0.324 ± 0.002 [b]	0.325 ± 0.004	0.321 ± 0.004 [b]	0.325 ± 0.011
Whole plasma membrane Limiting anisotropy	−	0.196 ± 0.003 [a,b]	0.213 ± 0.001 [a]	0.190 ± 0.004 [b]	0.201 ± 0.004
Inner anisotropy	+	0.212 ± 0.002 [b]	0.214 ± 0.003	0.206 ± 0.002 [b]	0.211 ± 0.007
Calculated (outer) monolayer limiting anisotropy		0.123 ± 0.003 [a]	0.211 ± 0.004 [a]	0.106 ± 0.005 [a]	0.169 ± 0.006 [a]
Ratio (outer/inner monolayer limiting anisotropy		0.58 ± 0.04 [a]	0.99 ± 0.004 [a]	0.51 ± 0.04 [a]	0.81 ± 0.04 [a]

[a] $P < 0.05$, as determined by Student's t-test, between F1 and F10.
[b] $P < 0.05$ ± TNBS.

with trinitrophenyl groups. More importantly, trinitrophenyl groups covalently linked to the outer monolayer of the plasma membrane completely quench the fluorescence of *trans*-parinarate, 1,6-diphenyl-1,3,5-hexatriene, dehydroergosterol and other fluorescent molecules in this monolayer [10,14–16,41,42]. Thus, from the limiting anisotropy of a fluorescent molecule in the untreated plasma membranes and in a plasma membrane containing covalently linked tritinitrophenyl groups in the outer monolayer, the limiting anisotropy of the probe can be calculated for both monolayers of the plasma membranes. When such procedures and calculations were performed with *trans*-parinaric acid and 1,6-diphenylhexatriene, the ratio of (outer/inner) limiting anisotropy was near 1.0, indicating the absence of a fluidity difference between the extracellular and cytoplasmic monolayer in the high metastatic B16-F10 plasma membrane (Table VI). In contrast, both probes showed a markedly decreased (outer/inner) ratio of 0.58 and 0.52, respectively ($P < 0.05$) in the low metastatic B16-F1 plasma membrane. The outer monolayer of B16-F1 plasma membranes thus appeared to offer less resistance to probe rotation than that of B16-F10 plasma membranes, as indicated by 42 and 38% smaller limiting anisotropy of *trans*-parinaric acid and 1,6-diphenylhexatriene, respectively, in the B16-F1 plasma membrane outer monolayer. No difference in rotational relaxation time of the probe molecules was noted between the two monolayers of either cell type. Fluorescence lifetime analysis may also be used to determine if all of the quenching sites are in or remain in the outer monolayer of the plasma membrane. Fluorescence quenching by energy transfer from *trans*-parinaric acid or 1,6-diphenylhexatriene to the trinitrophenyl group is expected to decrease the fluorescence lifetime of the probe molecules [47]. Since both of these fluorescent molecules were distributed across both monolayers of the plasma membranes, the fluorescence lifetime of the probe molecules in the whole membrane represents an intensity-weighted average of the lifetime of the probe in the inner plus outer monolayers. The fluorescence lifetime would then be expected to decrease upon energy transfer under the following conditions: (1) the outer monolayer was only partly quenched, or (2) if the outer monolayer was either partly or fully quenched and some of the quenching sites were in the inner monolayer (either from penetration of TNBS or from transbilayer migration of the quenching sites), or (3) if the inner monolayer were more mobile (had a smaller limiting anisotropy). The lifetime would be expected to remain unchanged or increased slightly if (1) the outer monolayer fluorescence were fully quenched, (2) there were no quenching sites in the inner monolayer, and (3) the inner monolayer was as rigid or more rigid than the outer monolayer. The data in Table VI indicated that the inner monolayer did not have a smaller limiting anisotropy; instead, the limiting anisotropy of the inner monolayer was equal to or greater than in the outer monolayer. In addition, the fluorescence lifetime of the probe molecules in the inner monolayer was either equal to or greater than that of the probe in the outer monolayer. Partial quenching, partial trinitrophenylation of the inner monolayer aminophospholipids, or transbilayer migration of quenching sites would all have led to a decrease in fluorescence lifetime. The data are not consistent with the occurrence of the latter events. These results were especially important, since they verified complete quenching of fluorescence of both probe molecules in the outer monolayer rather than partial quenching of one or both monolayers. Lastly, the absorbance-corrected fluorescence indicated that the majority of the fluorescence of *trans*-parinaric acid and 1,6-diphenylhexatriene originated from the inner monolayer. In both cases, up to 80 and 75%, respectively, of the fluorescence signal was located in the inner monolayer of the plasma membrane. However, since the inner monolayer was more rigid than the outer monolayer, this may contribute to a higher fluorescence efficiency of probe molecules in the inner monolayer and these percentages must therefore not be regarded as mole fractions or molar distributions of the probe molecules.

Thermal properties of trans-parinaric acid and 1,6-diphenylhexatriene in B16 melanoma membranes

Arrhenius plots of *trans*-parinarate or 1,6-diphenylhexatriene fluorescence in B16 melanoma membranes (Figs. 3 and 4) indicated the presence

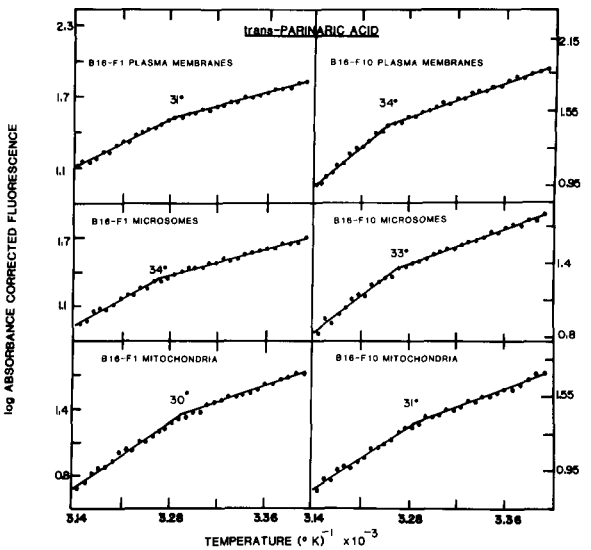

Fig. 3. Characteristic breakpoint temperatures in Arrhenius plots of *trans*-parinaric acid in B16 melanoma membranes. Plasma membranes, microsomes and mitochondria were isolated from B16-F10 and B16-F1 melanoma cells as described in Materials and Methods. The probe molecule *trans*-parinaric acid was incorporated into the membranes (50 μg protein/ml) and Arrhenius plots were performed on ascending temperature scans by the computer-centered fluorimeters as described in Materials and Methods.

of characteristic breakpoint temperatures. These characteristic temperatures may reflect phase alterations, changes in microdomains, or modifications in boundary lipid of proteins. Arrhenius plots of

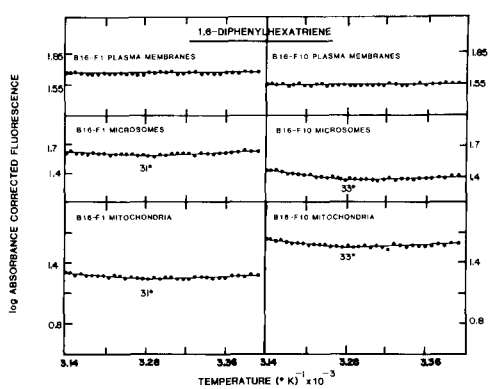

Fig. 4. Characteristic breakpoint temperatures in Arrhenius plots of 1,6-diphenylhexatriene in B16 melanoma membranes. All conditions were as specified in the legend to Fig. 3, except that 1,6-diphenylhexatriene was used instead of *trans*-parinaric acid.

trans-parinarate in both B16-F10 and B16-F1 melanoma plasma membranes, microsomes and mitochondria indicated the presence of similar breakpoints near 30–34°C (Fig. 3). Such breakpoints were also noted in microsomes and mitochondria but not in plasma membranes with 1,6-diphenyl-1,3,5-hexatriene (Fig. 4).

Since trinitrophenylation of the outer monolayer of the plasma membrane abolished the fluorescence of *trans*-parinarate or 1,6-diphenyl-1,3,5-hexatriene therein, and because the quenching sites remained on the outer surface after heating (see previous section), the transbilayer location of the characteristic breakpoint temperature may be ascertained. When the B16 melanoma cells were labeled with TNBS under nonpenetrating conditions (4°C), the *trans*-parinarate characteristic breakpoint temperature of the plasma membrane was still located near 32°C (Table VII), as were those of the microsomes and mitochondria. In contrast, under penetrating conditions (37°C), TNBS trinitrophenylated not only the outer but also the inner monolayer of the plasma membranes and thereby quenched almost all of the fluorescence. In addition, the microsomes and mitochondrial membranes are trinitrophenylated under penetrating conditions of 37°C. The penetrating conditions abolished the characteristic temperature in the plasma membranes as well as in most of the subcellular membranes (Table VII). These data are therefore consistent with an assignment of the characteristic breakpoint temperature near 30–34°C to the inner monolayer of the plasma membrane or to both monolayers having the same characteristic breakpoint temperature.

Discussion

A comparison of structural properties of membranes from high and low metastatic cell lines has previously not been reported. The data obtained with *trans*-parinaric acid indicated that the plasma membranes, microsomes and mitochondria of B16-F1 cells had a significantly lower ($P < 0.05$) limiting anisotropy than in the corresponding membranes from B16-F10 melanoma cells. In contrast, such differences were not noted with 1,6-diphenyl-1,3,5-hexatriene. These findings may be rationalized as follows. First, 1,6-diphenyl-1,3,5-

TABLE VII

CHARACTERISTIC TEMPERATURES IN ARRHENIUS PLOTS OF FLUORESCENCE PROBE MOLECULES IN B-16 MELANOMA MEMBRANES

Characteristic temperatures were determined from breakpoints in Arrhenius plots of absorbance-corrected fluorescence as described in Materials and Methods. Values represent the mean ± S.E. ($n = 3$ or 4). TNBS refers to trinitrobenzenesulfonate treatment of cells under the following conditions: none, nonpenetrating (4 °C), and penetrating (37 °C).

Cell fraction	Cell variants	Characteristic temperature (°C)		
		No TBNS	4 °C, TNBS	37 °C, TNBS
trans-Parinaric acid				
Plasma membrane	F1	31 ± 1	33 ± 1	none
	F10	34 ± 2	32 ± 1	none
Microsomes	F1	32 ± 1	33 ± 1	33 ± 1
	F10	31 ± 1	31 ± 1	34 ± 1
Mitochondria	F1	32 ± 1	33 ± 2	none
	F10	34 ± 2	32 ± 1	none
1,6-Diphenylhexatriene				
Plasma membrane	F1	none	none	none
	F10	none	none	none
Microsomes	F1	31 ± 1	31 ± 2	none
	F10	32 ± 1	32 ± 2	none
Mitochondria	F1	31 ± 2	33 ± 1	none
	F10	34 ± 1	32 ± 1	none

hexatriene partitions into both fluid and solid membrane areas nearly equally [27,28,30,48], and would therefore report on both fluid and solid areas of the membranes. In contrast, *trans*-parinaric acid demonstrated a nearly 4-fold preference for solid lipid areas [16,17,44,45] and would therefore report on solid membrane lipid behavior preferentially. Since approx. 24–37 mol% of the probe was located in solid domains (mole fraction X_2, Table II), one could therefore reason that 6–9% of the B16 melanoma membrane lipids were in the solid state at 24 °C. The *trans*-parinaric acid may therefore demonstrate that the solid lipid areas of the B16-F1 melanoma cell membranes were less rigid (shorter limiting anisotropy). This interpretation is also supported by the significant decrease of lifetime of *trans*-parinaric acid in the solid lipid areas, τ_2. The limiting anisotropy of both probe molecules was shorter in mitochondrial than in plasma membranes or microsomal membranes, indicating less hindrance to rotational motion in mitochondrial lipids. It should be noted that the rotational relaxation rates of the probe molecules were not significantly different in the various membranes. This finding is expected, since the rotational relaxation rate is not sensitive to membrane additives such as cholesterol, proteins, etc. [27,30,31]. The rotational relaxation rate of 1,6-diphenyl-1,3,5-hexatriene in B16 melanoma membranes was 1–2 ns, a value close to that obtained in model membrane systems [24].

In addition to the above observations, the finding that the B16-F1 melanoma plasma membrane solid domains may be more fluid (smaller limiting anisotropy) than those of the B16-F10 cell lines must be reconciled with previously noted lipid compositional changes [9]. Increased cholesterol/phospholipid ratio and small elevations in polyunsaturated fatty acid content were found in the B16-F1 whole cells, plasma membranes and microsomes as compared to B16-F10 membranes [9]. Elevations in cholesterol/phospholipid ratios would lead to increased limiting anisotropy (decrease fluidity), while increased polyunsaturated fatty acid content would expected to have the opposite effect. Biophysical determinations indicated that in the bulk fluid lipids, there was no difference in limiting anisotropy. Thus, the two effects must essentially cancel out. The data showing the presence of a more fluid solid lipid en-

vironment (lower *trans*-parinaric limiting anisotropy) in B16-F1 melanoma membranes is more difficult to rationalize, unless an altered lateral distribution of lipids between solid and fluid areas is invoked. Certainly, the transbilayer differences in structure are strickingly divergent between these cell lines (Table VI) and would lend support to postulation of transbilayer rearrangements of lipids as well.

The asymmetric distribution of aminophospholipid in both B16-F1 and B16-F10 melanoma cells was similar to that noted with another murine tumorigenic cell line, LM fibroblasts [33,34] and murine brain synaptosomes [35]. In addition, the transbilayer structure difference in B16-F1 plasma membranes was similar to that obtained with LM fibroblasts [10,41]. The decrease in this transbilayer ratio of (outer/inner) monolayer-limiting anisotropy could have considerable effects on protein exposure in the B16-F10 cells. Certainly, the exposure of $(Na^+ + K^+)$-ATPase, a transbilayer enzyme, and 5′-nucleotidase, an ecto-enzyme, to TNBS labelling was markedly different in the more rigid B16-F10 plasma membrane than in the B16-F1 plasma membranes (Table IV). The increased exposure of these proteins to TNBS could have been due to the lowered unsaturated/saturated fatty acid ratio in the B16-F10 plasma membranes. The effect of this lowered unsaturated fatty acid content may also be responsible in part for the abolition of the transbilayer fluidity difference in the B16-F10 plasma membranes.

Several pieces of data are consistent with indication of the presence of a characteristic temperature breakpoint in the inner monolayer of the plasma membrane. First, *trans*-parinaric acid Arrhenius plots showed breakpoints near 32°C. Second, since both B16-F1 and B16-F10 plasma membranes had the same breakpoint temperatures, one may expect that the limiting anisotropy of the probe molecules in the inner monolayer should not be significantly different between B16-F1 and B16-F10 melanoma plasma membranes. The data were consistent with this expectation. By analogy, since the limiting anisotropy of the probe molecules was markedly different in the outer monolayer of B16-F1 vs. B16-F10 plasma membranes, a different characteristic breakpoint temperature may be expected for outer monolayer lipids. The data, however, did not demonstrate such a difference. Third, when the fluorescence signal of the probe molecules in the outer monolayer was abolished by trinitrophenyl groups in the outer monolayer, the characteristic breakpoint temperature near 32°C was not altered. In contrast, when the fluorescence signal of 1,6-diphenylhexatriene was abolished in both monolayers, the characteristic breakpoint disappeared. Similar results were obtained with *trans*-parinaric acid, except in the case of the microsomes. This may be due to some of the *trans*-parinaric acid being inaccessible to the quenching agent. Indeed, approx. 10% of *trans*-parinarate may not be present in the lipid environment of some membranes and may be closely associated with protein in some membranes [43]. These results taken together with the data indicating a considerable difference in outer monolayer limiting anisotropy of probe molecules were consistent with the interpretation that such a characteristic breakpoint temperature was not present in the outer monolayer. Such a lack of a phase transition in one monolayer or different breakpoint temperatures in the two monolayers have been noted in other plasma membrane systems [49]. The rat-liver plasma membrane, for example, has a phase alteration in the outer but not the inner monolayer near 28°C [50–52]. Thus, not only the transbilayer fluidity gradient but the presence of two phases near physiological temperatures in at least one of the two monolayers of the plasma membranes may represent important potential modulators of transmembrane processes in metastatic cells.

One additional point relates to membrane structure and fluidity of membranes. Increased unsaturated fatty acid levels [9] of B16-F1 cells and the accompanying increased fluidity may enhance the heat-killing of these cells [53] and their complement-mediated cytolysis [54], perhaps accounting for their decreased metastatic properties. Other investigators have shown that the tumorigeneicity of a transformed cell line, FK 3T3, decreased with increasing polyunsaturated fatty acid content and with increased cholesterol/phospholipid ratio [55]. These findings were consistent with lipid differences noted between low metastatic B16-F1 and high metastatic B16-F10 melanoma cells [7] in which a higher polyun-

saturated fatty acid content was demonstrated for B16-F1 cells compared to B16-F10 cells. Increased fludity of CHO cells decreased the adherence of the cells to protein-coated substrates [7]. This finding may also account for the lowered formation of metastatic sites by the more fluid B16-F1 than the less fluid B16-F10 melanoma cells. These results correlating higher membrane fluidity with higher polyunsaturated fatty acid content and with lower metastatic incidence must be extrapolated to other tumor cells with caution. Certainly, a simple extrapolation of these properties for metastatic potential to those of oncogenic potential is not appropriate. Indeed, other investigations correlated increased fluidity in whole cells of a series of chemically transformed $C_3H10T_{1/2}CL8$ cell lines [8] and ascites cell lines [56] with increased oncogenicity or tumorigenicity. The latter finding may relate to primary tumors rather than to metastasis formation. In either case, more data on other high vs. low metastatic cell lines and their isolated membrane fluidity rather than whole cell fluidity must be obtained before any generalization may be made. Whole cell fluidity determinations are especially prone to provide data that prevent definitive conclusions [57].

In conclusion, the structure of isolated plasma membranes from high and low metastatic B16 melanoma variants differed markedly. Plasma membranes from high metastatic B16-F10 melanoma cells had similar bulk fluidity (except for solid lipid domains) than those of the low metastatic B16-F1 melanoma cells. However, the transbilayer fluidity difference prominent in the low metastatic B16-F1 melanoma plasma membrane was essentially absent in the high metastatic B16-F10 melanoma plasma membrane. Such a transbilayer fluidity difference in which the inner monolayer of the plasma membrane is more rigid than the outer monolayer was also established in the tumorigenic LM fibroblast plasma membrane [10,41]. This cell line metastasized poorly in normal C_3H/Hen mice, although, in athymic nude mice, it metastasized efficiently [46]. These findings may represent an important advance in our understanding of the metastatic process,since they point out subtle rather than gross alterations in membrane structure.

Acknowledgement

The author wishes to thank Dr. E.M. Jensen of the EG&G Mason Research Institute, Worcester, MA, and Dr. Isaiah J. Fidler of the Frederick Cancer Research Center (Frederick, MD) for the gift of the B16-F10 and B16-F1 melanoma cell lines. The helpful advice of Dr. Jane Berkelhammer, Sinclair Research Farms, University of Missouri, on culturing of these cells was much appreciated. Also, we wish to acknowledge the expert technical assistance of Mr. Jack Gardiner and Mr. Jon Waters for culturing the cells and Mr. Eugene Hubert in performing the fluorescence experiments, and Mrs Genie Eckenfels and Mrs. Doris Estes for preparing the manuscript. This investigation was supported primarily by a grant from the USPHS (CA 24339) and, in part, by grant GM 31651.

References

1 Poste, G. and Fidler, I.J. (1980) Nature 283, 139–146
2 Fidler, I.J., Gersten, D.M. and Hart, I.R. (1978) Adv. Cancer Res. 28, 149–250
3 Poste, G. (1980) Biochem. Soc. Trans. 8, 695–697
4 Levine, L. (1981) Adv. Cancer Res. 35, 49–79
5 Stringfellow, D.A. and Fitzpatrick, F.A. (1979) Nature (Lond.) 282, 76–78
6 Carley, W.W., Barak, L.S. and Webb, W.W. (1982) J. Cell Biol. 90, 797–802
7 Juliano, R. and Gagalong, E. (1979) Am. J. Physiol. 98: 483–490
8 Monti, J.A., Sarrif, A.M., Christian, S.T. and Saxholm, H.J.K. (1979) Arch. Biochem. Biophys. 193, 496–501
9 Schroeder, F. and Gardiner, J. (1984) Cancer Res. 44, 3262–3269
10 Schroeder, F. (1980) Eur. J. Biochem. 112, 293–307
11 Holland, J.F., Teets, R.E. and Timnick, A. (1973) Anal. Chem. 45, 145–153
12 Holland, J.F., Teets, R.E., Kelly, P.M. and Timnick, A. (1977) Anal. Chem. 49, 706–710
13 Christmann, D.R., Crouch, S.R., Holland, J.F. and Timnick, A. (1980) Anal. Chem. 52, 291–295
14 Schroeder, F. and Goh, E.H. (1979) J. Biol. Chem. 254, 2464–2470
15 Schroder, F., Goh, E.H. and Heimberg, M. (1979) J. Biol. Chem. 254, 2456–2463
16 Schroeder, F. (1983) Eur. J. Biochem. 132, 509–516
17 Schroeder, F. and Soler-Argilaga, C. (1983) Eur. J. Biochem. 132, 517–524
18 Weber, G. and Bablouzian, B. (1966) J. Biol. Chem. 241, 2558–2561

19 Hale, J.E. and Schroeder,F. (1982) Eur. J. Biochem. 122, 649–661
20 Lentz, B.R., Moore, B.M. and Barrow, D.A. (1979) Biophys. J. 25, 489–494
21 Chong, C.S. and Colbow, K. (1976) Biochim. Biophys. Acta 436, 260–282
22 Lakowicz, J.R., Cherek, H. and Balter, A. (1981) J. Biochem. Biophys. Methods 5, 131–146
23 Weber, G. (1981) J. Phys. Chem. 85, 949–953
24 Lakowicz, J.R., Prendergast, F.G. and Hogen, D. (1979) Biochemistry 18, 508–519
25 Weber, G. (1953) Adv. Protein Chem. 8, 415–459
26 Shinitzky, M. and Inbar, M. (1974) J. Mol. Biol. 85, 603–615
27 Kinosita, K., Kataoka, R., Kimura, Y., Gotoh, O. and Ikegami, A. (1981) Biochemistry 20, 4270–4277
28 Kawato, S., Kinosita, K. and Ikegami, A. (1979) Biochemistry 16, 2319–2324
29 Wolber, P.K. and Hudson, B.S. (1981) Biochemistry 20, 2800–2810
30 Jahnig, F., Vogel, H. and Best, L. (1982) Biochemistry 21, 6790–6798
31 Jahnig, F. (1979) Proc. Natl. Acad. Sci. USA 76, 6361–6365
32 Weber, G. (1952) Biochem. J. 51, 145–167
33 Fontaine, R.N. and Schroeder, F. (1979) Biochim. Biophys. Acta 558, 1–12
34 Schroeder, F. (1980) Biochim. Biophys. Acta 599, 254–270
35 Fontaine, R.N., Harris, R.A. and Schroeder, F. (1980) J. Neurochem 34, 269–277
36 Schroeder, F. (1982) J. Membrane Biol. 68, 141–150
37 Sandra, A. and Pagano, R.E. (1978) Biochemistry 17, 332–338
38 Gordesky, S.E., Marinetti, G.V. and Segel, G.B. (1972) Biochem. Biophys. Res. Commun. 47, 1004–1009
39 Litman, B.J. (1974) Biochemistry 13, 2844–2848
40 Smith, H.G., Fager, R.S. and Litman, B.J. (1977) Biochemistry 16, 1399–1405
41 Schroeder, F. (1978) Nature (Lond.) 275, 528–530
42 Schroeder, F. (1981) FEBS Lett. 135, 127–130
43 Schroeder, F., Holland, J.F. and Vagelos, P.R. (1976) J. Biol. Chem. 251, 6739–6746
44 Sklar, L.A., Hudson, B.S. and Simoni, R.D. (1977) Biochemistry 16, 819–828
45 Sklar, L.A., Miljanich, G.P. and Dratz, E.A. (1979) Biochemistry 18, 1707–1716
46 Kier, A.B. and Schroeder, F. (1982) Transplantation 33, 274–279
47 Radda, G.K. (1975) in Methods in Membrane Biology, Vol. 4, Biophysical Approaches (Korn, E.D., ed.), pp. 97–188, Plenum Press, New York
48 Andrich, M.P. and Vanderkooi, J.M. (1976) Biochemistry 15, 1257–1261
49 Wisnieski, B.J. and Iwata, K.K. (1977) Biochemistry 16, 1321–1326
50 Dipple, I. and Houslay, M.D. (1978) Biochem. J. 174, 179–190
51 Houslay, M.D., Hesketh, T.R., Smith, G.A., Warren, G.B. and Metcalfe, J.C. (1976) Biochim. Biophys. Acta 436, 495–504
52 Sauerheber, R.D., Gordon, L.M., Crosland, R.D. and Kuwahara, M.D. (1977) J. Membrane Biol. 31, 131–169
53 Hidvegi, E.J., Yatvin, M.B., Dennis, W.H. and Hidvegi, E. (1980) Oncology 37, 360–363
54 Yoo, T.-J., Chiu, H.C., Spector, A.A., Whiteaker, R.S., Denning, G.M. and Lee, N.F. (1980) Cancer Res. 40, 1084–1090
55 Corwin, L.M., Varshavsky-Rose, F. and Broitman, S.A. (1979) Cancer Res. 39, 4350–4355
56 Haeffner, E.W., Heck, B. and Kolbe, K. (1982) Biochim. Biophys. Acta 693, 280–286
57 Esko, J.D., Gilmore, J.R. and Glaser, M. (1977) Biochemistry 16, 1881–1890